

# Large-scale dynamo action of magnetized Taylor-Couette flows

G. Rüdiger<sup>1,2\*</sup>, M. Schultz<sup>1</sup>,

<sup>1</sup>Leibniz-Institut für Astrophysik Potsdam, An der Sternwarte 16, 14482 Potsdam, Germany

<sup>2</sup>University of Potsdam, Institute of Physics and Astronomy, Karl-Liebknecht-Str. 24-25, 14476 Potsdam, Germany

Accepted . Received ; in original form

## ABSTRACT

A conducting Taylor-Couette flow with quasi-Keplerian rotation law containing a toroidal magnetic field serves as a mean-field dynamo model of the Tayler-Spruit-type. The flows are unstable against nonaxisymmetric perturbations which form electromotive forces defining  $\alpha$  effect and eddy diffusivity. If both degenerated modes with  $m = \pm 1$  are excited with the same power then the global  $\alpha$  effect vanishes and a dynamo cannot work. It is shown, however, that the Tayler instability produces finite  $\alpha$  effects if only an isolated mode is considered but this intrinsic helicity of the single-mode is too low for an  $\alpha^2$  dynamo. Moreover, an  $\alpha\Omega$  dynamo model with quasi-Keplerian rotation requires a minimum magnetic Reynolds number of rotation of  $Rm \simeq 2.000$  to work. Whether it really works depends on assumptions about the turbulence energy. For a steeper-than-quadratic dependence of the turbulence intensity on the magnetic field, however, dynamos are only excited if the resulting magnetic eddy diffusivity approximates its microscopic value,  $\eta_T \simeq \eta$ . By basically lower or larger eddy diffusivities the dynamo instability is suppressed.

**Key words:** Magnetohydrodynamics – Tayler instability – dynamo theory

## 1 INTRODUCTION

A Taylor-Couette flow with a smooth rotation profile beyond the Rayleigh limit becomes unstable if the magnetic background field is toroidal (or has a toroidal component) for relatively low critical Reynolds numbers. If the magnetic field is strictly axial then the Reynolds numbers necessary for instability are higher by several orders of magnitude if the magnetic Prandtl number  $Pm = \nu/\eta$  (with  $\nu$  the molecular viscosity and  $\eta$  the molecular resistivity) is much smaller than unity. The reason is that the instabilities set in at fixed Reynolds number for toroidal background fields and at fixed magnetic Reynolds number for axial background fields which basically differ for  $Pm \ll 1$ .

On the other hand, the critical Reynolds number is even zero if the toroidal magnetic field is not current-free in the gap between the cylinders and the electric current is strong enough (Tayler 1957). The critical amplitudes of the toroidal field form a characteristic Hartmann number which for resting flows only depends on the radial profile of the field not on the magnetic Prandtl number. It takes its minimum if the field is due to an axial electric current which is homogeneous in the container. Moreover, the Tayler instability is suppressed by the rotation (Pitts & Tayler 1985). As a consequence, a rotating magnetized Couette flow can only be unstable for supercritical magnetic fields where to all supercritical Hartmann numbers a maximal Reynolds number belongs above which the instability decays. This line of neutral stability and the instability line for nonrotating flows form a domain of unstable flows as in the left

panel of Fig. 1) which can be probed for their ability to transport angular momentum, to diffuse chemicals, dissipate magnetic fields and/or to form helicity and even  $\alpha$  effect (Rüdiger et al. 2018).

Flows of the Chandrasekhar-type, where the background field and the background flow have identical isolines, are unstable against nonaxisymmetric perturbations if at least one of the diffusivities is non-zero. For  $Pm \ll 1$  the onset of the instability also scales with the Reynolds number and the Hartmann number, i.e. the neutral stability curves converge for  $Pm \rightarrow 0$  in the Hartmann number/Reynolds number plane. A prominent example of this class of magnetohydrodynamic flows is the axially unbounded rigidly rotating  $z$ -pinch exhibiting toroidal flows and fields which only vary with the distance  $R$  from the rotation axis. The condition

$$\frac{d}{dR}(RB_\phi^2) \leq 0 \quad (1)$$

is sufficient and necessary for stability of a stationary ideal fluid against nonaxisymmetric perturbations (Tayler 1973). As a consequence, one finds uniform or outwardly increasing magnetic fields unstable against nonaxisymmetric perturbations. This is in particular true for the field with  $B_\phi \propto R$  produced by a uniform electric current. The existence of the nonaxisymmetric instability for such a nonrotating ‘ $z$ -pinch’ has experimentally been shown by Seilmayer et al. (2012) using liquid GaInSn as the conducting fluid penetrated by an axial electric current.

The Tayler instability in rotating Couette flows and its qualification to induce mean-field electromotive forces shall here be considered to question its dynamo activity. It has been suggested that the combination of axisymmetric differential rotation and nonaxisymmetric Tayler instability patterns may work as a dy-

\* E-mail: GRuediger@aip.de

namo in the convectively stable radiative interiors of stars (Spruit 2002). Numerical simulations by Braithwaite (2006) seem to realize such a dynamo model but so far its existence is still under debate (Gellert et al. 2008; Zahn et al. 2007; Goldstein et al. 2019). In the present paper we shall attack the problem by use of a mean-field dynamo formulation considering a simple  $z$ -pinch model subject to differential rotation. The flows and fields are assumed as unbounded in the axial direction and the related instabilities are always nonaxisymmetric. We are here formulating a linear theory for the onset of a possible dynamo and ignore all consequences of its nonlinear evolution. The main result will be that only the assumptions about the numerical values of the Tayler-induced resistivity in its dependencies on magnetic field and rotation will decide whether a dynamo self-excitation is possible or not.

By numerical simulations dynamo excitation on the basis of the azimuthal magnetorotational instability (AMRI) of quasi-Keplerian flow has been shown by Guseva et al. (2017). Due to the large magnetic Prandtl number  $\text{Pm} = 10$  the magnetic energy approaches the kinetic energy which might be a condition of small-scale magnetohydrodynamic dynamo processes. In order to avoid the operation of a small-scale dynamo mainly  $\text{Pm} = 0.1$  is used in the present paper while smaller values would be beyond the limitations of our numerical calculations. In contrast to applications with AMRI the azimuthal background field of the Tayler instability is due to a large-scale axial electric current  $\mathbf{J}$ . A pseudoscalar  $\mathbf{B} \cdot \mathbf{J}$  can thus be formed so that an  $\alpha$  effect – known from the mean-field dynamo theory – may exist. Note that the global rotation  $\Omega$  is not needed for this argumentation and that for AMRI with its  $\mathbf{J} = 0$  such a pseudoscalar does not exist at all.

The outline of the paper is as follows. Section 2 presents the magnetohydrodynamic equation system which governs the problem. The boundary conditions are given for both insulating and perfect-conducting cylinders. Section 3 deals with the linear eigenvalue problem of the pinch-type instability where the toroidal field is assumed as due to a homogeneous and axial electric current between the cylindrical walls. The components of the instability-induced electromotive force are calculated in Section 4 including an  $\alpha$  effect which only appears for a single-mode but vanishes if the complete spectrum of the modes is considered. A mean-field dynamo model is constructed in Section 5 where by the small value of the resulting helicity the operation of  $\alpha^2$  dynamos can immediately be excluded. Section 6 combines the microscopic and the macroscopic results leading to the conclusion that an  $\alpha\Omega$  dynamo mechanism is only possible if for the needed fast rotation the instability-induced diffusivity is strongly reduced.

## 2 THE EQUATIONS

The equations of the problem are the standard equations of magnetohydrodynamics,

$$\begin{aligned} \frac{\partial \mathbf{U}}{\partial t} + (\mathbf{U} \cdot \nabla) \mathbf{U} &= -\frac{1}{\rho} \nabla P + \nu \Delta \mathbf{U} + \frac{1}{\mu_0 \rho} \text{curl} \mathbf{B} \times \mathbf{B}, \\ \frac{\partial \mathbf{B}}{\partial t} &= \text{curl}(\mathbf{U} \times \mathbf{B}) + \eta \Delta \mathbf{B} \end{aligned} \quad (2)$$

with  $\text{div} \mathbf{U} = \text{div} \mathbf{B} = 0$  for an incompressible magnetized fluid of density  $\rho$ .  $\mathbf{U}$  is the velocity,  $\mathbf{B}$  the magnetic field and  $P$  the pressure. The basic state in the cylindrical system with the coordinates  $(R, \phi, z)$  is  $U_R = U_z = B_R = B_z = 0$  for the poloidal com-

ponents and

$$\Omega = a + \frac{b}{R^2} \quad (3)$$

for the rotation law with  $a$  and  $b$  as constants.  $r_{\text{in}} = R_{\text{in}}/R_{\text{out}}$  be the ratio of the inner cylinder radius  $R_{\text{in}}$  and the outer cylinder radius  $R_{\text{out}}$  while  $\Omega_{\text{in}}$  and  $\Omega_{\text{out}}$  are the angular velocities of the inner and outer cylinders, respectively. With the definition  $\mu = \Omega_{\text{out}}/\Omega_{\text{in}}$ , sub-rotation (negative shear,  $d\Omega/dR < 0$ ) is represented by  $\mu < 1$  and super-rotation (positive shear,  $d\Omega/dR > 0$ ) by  $\mu > 1$ . The absolute shear value  $|d\Omega/dR|$  may monotonously sink from the inner cylinder to the outer cylinder. We shall work in this paper with uniform rotation ( $\mu = 1$ ) as well as with a quasi-Keplerian rotation law ( $\mu = r_{\text{in}}^{3/2}$ ) where the inner and the outer cylinder rotate like planets.

The two  $z$ -independent solutions of (2) for the magnetic background field  $B_\phi$  are  $R$  and  $1/R$  where the latter is current-free in the fluid. We define  $\mu_B = B_{\text{out}}/B_{\text{in}}$ . Only the pinch-type solution with  $B_\phi = B_{\text{in}}R/R_{\text{in}}$  is here considered, i.e.  $\mu_B = 1/r_{\text{in}}$ .

The dimensionless physical parameters of the system besides the magnetic Prandtl number  $\text{Pm}$  are the Hartmann number  $\text{Ha}$  and the Reynolds number  $\text{Re}$

$$\text{Ha} = \frac{B_{\text{in}} D}{\sqrt{\mu_0 \rho \nu \eta}}, \quad \text{Re} = \frac{\Omega_{\text{in}} D^2}{\nu} \quad (4)$$

where the inner magnetic field and the rotation rate of the inner cylinder are used. The difference  $D = R_{\text{out}} - R_{\text{in}}$  is the gap width between the cylinders. The magnetic Lundquist number is  $\text{S} = \sqrt{\text{Pm}} \cdot \text{Ha}$ .

The variables  $\mathbf{U}$ ,  $\mathbf{B}$  and  $P$  are split into mean and fluctuating components, i.e.  $\mathbf{U} = \bar{\mathbf{U}} + \mathbf{u}$ ,  $\mathbf{B} = \bar{\mathbf{B}} + \mathbf{b}$  and  $P = \bar{P} + p$ . The bars of the variables are immediately dropped so that the capital letters  $\mathbf{U}$ ,  $\mathbf{B}$  and  $P$  represent the background quantities. By developing the disturbances  $\mathbf{u}$ ,  $\mathbf{b}$  and  $p$  into normal modes,

$$[\mathbf{u}, \mathbf{b}, p] = [\mathbf{u}(R), \mathbf{b}(R), p(R)] \exp(i(\omega t + kz + m\phi)), \quad (5)$$

the solutions of the linearized MHD equations are constructed for axially unbounded cylinders. Here  $k$  is the axial wave number of the perturbation,  $m$  its azimuthal wave number and  $\omega$  the complex frequency including growth rate as its negative imaginary part and a drift frequency  $\omega_{\text{dr}}$  as its real part. A linear code is used to solve the resulting set of linearized ordinary differential equations for the radial functions of flow, field and pressure fluctuations. The ratio  $\eta/D$  serves as the unit of the velocity,  $B_{\text{in}}$  as the unit of the field perturbations and  $\Omega_{\text{in}}$  as the unit of frequencies. The solutions are optimized with respect to the Reynolds number for given Hartmann number by varying the wave number. Only solutions for  $m = \pm 1$  are here discussed. The hydrodynamic boundary conditions at the cylinder walls are the rigid ones, i.e.  $u_R = u_\phi = u_z = 0$ . The cylinders are often assumed to be perfectly conducting. For the conducting walls the fluctuations  $\mathbf{b}$  must fulfill  $db_\phi/dR + b_\phi/R = b_R = 0$  at  $R_{\text{in}}$  and  $R_{\text{out}}$  so that ten boundary conditions exist for the set of ten differential equations. The magnetic boundary conditions for insulating walls are

$$b_R + \frac{ib_z}{I_m(kR)} \left( \frac{m}{kR} I_m(kR) + I_{m+1}(kR) \right) = 0 \quad (6)$$

for  $R = R_{\text{in}}$ , and

$$b_R + \frac{ib_z}{K_m(kR)} \left( \frac{m}{kR} K_m(kR) - K_{m+1}(kR) \right) = 0 \quad (7)$$

for  $R = R_{\text{out}}$ , where  $I_m$  and  $K_m$  are the modified Bessel functions of second kind. The conditions for the toroidal field are simply  $kRb_\phi = m b_z$  at  $R_{\text{in}}$  and  $R_{\text{out}}$ . Details including the modified

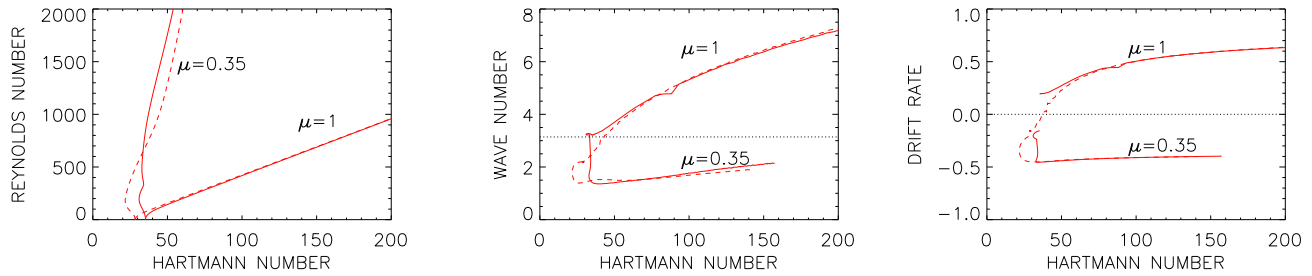


**Figure 1.** Left: Stability maps of the  $z$ -pinch subject to rigid rotation ( $\mu = 1$ ) and for quasi-Keplerian rotation ( $\mu = 0.35$ ). The areas below the lines of neutral stability mark the unstable domains. Middle: Normalized wave numbers along the lines of neutral stability. The values above (below) the horizontal dotted line provide oblate (prolate) cell structures. Right: Drift rates in units of the inner cylinder rotation along the lines of neutral stability.  $r_{\text{in}} = 0.5$ ,  $\mu_B = 2$ ,  $m = \pm 1$ ,  $\text{Pm} = 0.1$ . Perfect-conducting boundary conditions (solid lines), insulating boundary conditions (dashed lines).

expressions for cylinders with finite electric conductivity are given by Rüdiger et al. (2018).

### 3 PINCH-TYPE INSTABILITY

The combination of the magnetic field  $B_\phi \propto R$  and the rigid-rotation profile  $\Omega = \text{const}$  belongs to a particular class of MHD flows defined by Chandrasekhar (1956) as  $\mathbf{U} = \mathbf{U}_A$ . The radial profiles of flow velocity  $\mathbf{U}$  and Alfvén velocity  $U_A = \mathbf{B}/\sqrt{\mu_0\rho}$  are here identical. All such flows are stable in the absence of diffusive effects. The rigidly rotating  $z$ -pinch belongs to the class of the Chandrasekhar-type flows as both the toroidal magnetic profile and the linear velocity linearly run with  $R$ . This implies a uniform axial electric current throughout the entire region  $R < R_{\text{out}}$ . For all fluids of the Chandrasekhar-type in the  $(\text{Ha}/\text{Re})$  plane the lines of marginal stability for  $m = \pm 1$  converge for  $\text{Pm} \rightarrow 0$ .

#### 3.1 Stability maps

The curves of neutral instability for  $m = \pm 1$  and the two rotation laws (rigid and quasi-Keplerian rotation) are shown in the left panel of Fig. 1 for both perfectly conducting and insulating boundaries. The resulting instability is purely current-driven. Such instabilities even exist for  $\text{Re} = 0$  for supercritical Hartmann numbers  $\text{Ha} \geq \text{Ha}_0$ . The given curves demonstrate the stabilizing effect of the global rotation so that for all  $\text{Ha} \geq \text{Ha}_0$  maximal Reynolds numbers  $\text{Re}_{\text{max}}$  exist. The curves of the maximal Reynolds numbers become the more steep the smaller the magnetic Prandtl number is. The rotational suppression is thus strongest for  $\text{Pm} = 1$ , it becomes weaker for smaller magnetic Prandtl numbers. For rigid rotation and for quasi-Keplerian rotation it has been shown that for highly supercritical Hartmann numbers the maximal Reynolds number grows with growing Hartmann number. For small  $\text{Pm}$  and slow rotation also subcritical excitations are possible.

Figure 1 also shows the minor importance of the boundary conditions for shape and extension of the instability domains. The rotational stabilization of the nonaxisymmetric instability for differential rotation is much weaker than for rigid rotation. Above the lines the flow is stable. The limiting Reynolds number depends on the magnetic Prandtl number, i.e. the smaller  $\text{Pm}$  the higher the maximal Reynolds number for the instability. For Chandrasekhar-type flows, however, the  $\text{Re}_{\text{max}}$  lose their  $\text{Pm}$ -dependence if  $\text{Pm} \rightarrow 0$ . This is of course not true for a quasi-Keplerian flow which allows instability up to  $\text{Re}_{\text{max}} \simeq 1000$  for  $\text{Pm} = 1$  and up

to  $\text{Re}_{\text{max}} \simeq 8812$  for  $\text{Pm} = 10^{-5}$  (both for  $\text{Ha} = 50$ ). Hence, the  $\text{Pm}$ -dependence of the maximal Reynolds number is as weak as  $\text{Re}_{\text{max}} \propto \text{Pm}^{-0.16}$  for fixed Hartmann number and for small  $\text{Pm}$  while this dependence vanishes for Chandrasekhar-type flows with  $\text{Pm} \rightarrow 0$ .

The middle and right panels of Fig. 1 present the normalized wave numbers  $kD$  and the normalized drift frequencies  $\omega/\Omega_{\text{in}}$  along the lines of neutral instability. The middle panel shows that the shape of the cells depends on the form of the rotation law. While for rigid rotation the cells are quite oblate they are prolate for the quasi-Keplerian rotation. For stronger magnetic fields the wave numbers monotonously grow. For our two rotation laws the azimuthal drift rate even possesses opposite signs. Again the influence of the boundary conditions is only weak.

The shape of the stability lines in the  $(\text{Ha}/\text{Re})$  plane can be expressed by the magnetic Mach number  $\text{Mm} = \text{Rm}/S$ , i.e.

$$\text{Mm} = \frac{\sqrt{\text{Pm}} \text{Re}_{\text{max}}}{\text{Ha}}, \quad (8)$$

which for the quasi-Keplerian flow clearly exceeds the value for rigid rotation by one order of magnitude (Fig. 2). For the latter case there is almost no dependence of the curves on the magnetic Prandtl number. A weak dependence exists for differential rotation: the magnetic Mach number varies by one or two orders of magnitude for magnetic Prandtl numbers varying by four orders of magnitude. Only the non-uniform rotation in combination with the larger  $\text{Pm}$  leads to superAlfvénic values of the  $\text{Re}_{\text{max}}$ , as expected because of enhanced induction in the high-conductivity limit.

The key question for the existence of  $\alpha\Omega$  dynamos of the Taylor-Spruit-type will be whether the described rotational quenching still allows rotation rates which are high enough for dynamo excitation driven by the flow and field perturbations. Also the question arises whether even flows with positive shear ( $\mu > 1$ ) may operate as a large-scale dynamo. The Taylor instability under the presence of super-rotation is also suppressed for fast rotation so that the differences to systems with sub-rotation might be small. For slow rotation the instability is magnetically supported so that for  $\text{Pm} \neq 1$  subcritical excitations appear (Kirillov et al. 2012; Rüdiger et al. 2018). As we shall see, however, the large-scale dynamo only operates in the fast-rotation limit.

#### 3.2 Eigensolutions

The homogeneous system of differential equations for the perturbations forms an eigenvalue problem with eigensolutions for  $\mathbf{u}(R)$

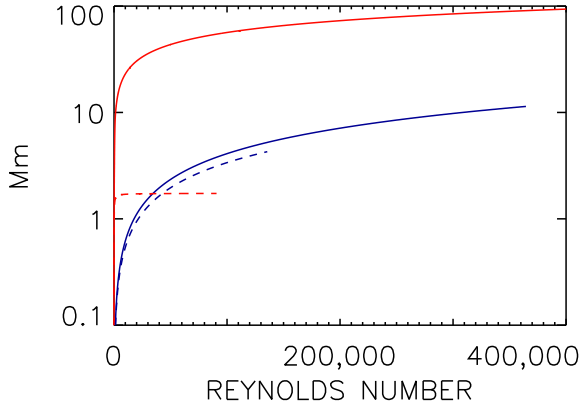


**Figure 2.** Magnetic Mach number (8) versus Reynolds number  $\text{Re}_{\text{max}}$  along the lines of marginal stability for quasi-Keplerian rotation and for  $\text{Pm} = 0.1$  (red line) and  $\text{Pm} = 10^{-5}$  (blue). The dashed curves are for rigid rotation. Perfect-conducting boundary conditions.

and  $\mathbf{b}(R)$  which can be determined up to a free real multiplication factor. For  $m = \pm 1$  the components  $u_R, u_\phi, b_R$  and  $b_\phi$  are conjugate-complex as also the field components  $-iu_z$  and  $-ib_z$  are. It means that for the transformation  $m \rightarrow -m$  the components  $b_R$  (and  $b_\phi$ ) transform as  $b_R^R \rightarrow b_R^R$  and  $b_R^I \rightarrow -b_R^I$  while for the same transformation  $b_z^R \rightarrow -b_z^R$  and  $b_z^I \rightarrow b_z^I$ . The superscripts R stand for the real parts and I for the imaginary parts of the eigensolutions  $\mathbf{u}$  and  $\mathbf{b}$ . These transformation rules lead to opposite behaviors of the calculated components of the electromotive force (such as  $\alpha$  effect and eddy resistivity) if both modes are excited.

The product of two scalars  $A$  and  $B$  after averaging over the  $\phi$  coordinate is the sum of the products of the real parts and the imaginary parts, i.e.  $AB = A^R B^R + A^I B^I$ . There is a certain factor in front of this expression whose value, however, is unimportant as in the linear theory the vector components are only known up to a free factor. It is thus clear that in the linear theory only *ratios* of second-order correlations (auto-correlations or cross-correlations) can be calculated which are free of the arbitrary parameter.

We shall understand the averaging rules as summation of all values located on a cylinder of radius  $R$ . The results are independent of  $\phi$  and  $z$ . This procedure will first be applied to the ratio

$$\varepsilon = \frac{\langle \mathbf{b}^2 \rangle}{\mu_0 \rho \langle \mathbf{u}^2 \rangle} \quad (9)$$

of the magnetic and kinetic energy. We shall calculate these values as averages over the whole container along the stability curves  $\text{Re}_{\text{max}} = \text{Re}_{\text{max}}(\text{Ha})$  of the left panel of Fig. 1. In dimensionless quantities it is  $\varepsilon = S^2 \langle \mathbf{b}^2 \rangle / \langle \mathbf{u}^2 \rangle$ .

Figure 3 gives the results in form of  $\varepsilon/\text{Pm}$ . For small  $\text{Pm}$  also the magnetic energy is very small compared with the kinetic one, i.e.  $b_{\text{rms}} \simeq \sqrt{\mu_0 \rho \text{Pm}} u_{\text{rms}}$ . The Maxwell stress for  $\text{Pm} \ll 1$ , therefore, will not play an important role in diffusion processes such as angular momentum transport or turbulent decay of fossil magnetic fields. One finds, however, that for differential (Kepler) rotation and larger magnetic Prandtl numbers the magnetic energy indeed exceeds the kinetic one. The solid red line in the plot (for quasi-Keplerian rotation and  $\text{Pm} = 0.1$ ) clearly demonstrates the generation of magnetic fluctuations by differential rotation for large  $\text{Pm}$ , i.e. for large microscopic electric conductivity.

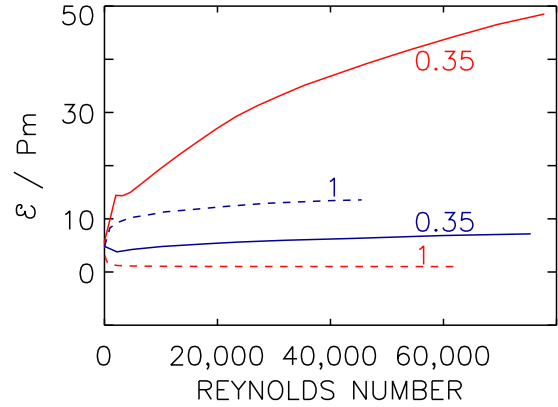


**Figure 3.** Ratio  $\varepsilon$  after (9) divided by the magnetic Prandtl number along the line of neutral stability ( $\text{Re} = \text{Re}_{\text{max}}$ ) for the pinch with rigid rotation (dashed lines) and with quasi-Keplerian rotation (solid lines). The curves are marked with their values of  $\mu, r_{\text{in}} = 0.5, \mu_B = 2, m = \pm 1, \text{Pm} = 0.1$  (red) and  $\text{Pm} = 10^{-5}$  (blue). Perfect-conducting boundary conditions.

One also finds that for differential rotation the  $\varepsilon$  slightly grows with the Reynolds number along the line of neutral stability. As expected, the magnetic energy exceeds the kinetic energy the more the faster the rotational shear but this effect is not too strong. The energy ratio  $\varepsilon$  in this case runs as  $\varepsilon \propto \text{Pm}^{0.85} \text{Rm}^{0.35}$ . This expression strongly grows with growing electric conductivity indicating the important role of the shear-originated induction.

#### 4 ELECTROMOTIVE FORCE

Next the axisymmetric part of the electromotive force  $\mathcal{E} = \langle \mathbf{u} \times \mathbf{b} \rangle$  is considered which is due to the correlations of flow and field perturbations. We first proceed again along the lines of neutral stability in Fig. 1 (left) because a possible dynamo will work much easier for fast rotation than for slow rotation. The line of neutral stability defines the maximally possible rotation rates belonging to a given magnetic field. Below this line the rotation is slower so that for dynamo excitation the  $\alpha$  effect must be larger.

By proper normalizations the influence of the unknown free factor can be eliminated. Again the averaging procedure concerns the time and the coordinates  $\phi$  and  $z$ . The mean-field electromotive force may be developed in the series

$$\mathcal{E} = \alpha \mathbf{B} - \eta_T \text{curl} \mathbf{B} + \dots \quad (10)$$

with the  $\alpha$  effect and the eddy diffusivity  $\eta_T$  as coefficients of the large-scale field and the large-scale electric current which both are nontrivial tensors. In cylinder geometry, the  $\phi$ -component  $\mathcal{E}_\phi = \langle u_z b_R - u_R b_z \rangle$  can be written as the axisymmetric part of expressions such as  $\langle u_z b_R \rangle \propto u_z^R b_R^R + u_z^I b_R^I$ . Because of the different transformation rules for radial and axial components of the eigenvectors the expression  $\mathcal{E}_\phi$  takes opposite signs for  $m \rightarrow -m$ . It is thus evident that the total azimuthal electromotive force due to the instability of azimuthal fields vanishes if both modes  $m$  and  $-m$  (which have the same eigenvalues and the same azimuthal drifts) are simultaneously excited with the same power. Only by an extra parity braking (e.g. by an additional  $z$ -component of the magnetic background field) finite values of the  $\alpha$  effect appear. Another possibility is to consider the isolated modes  $m = 1$  and  $m = -1$

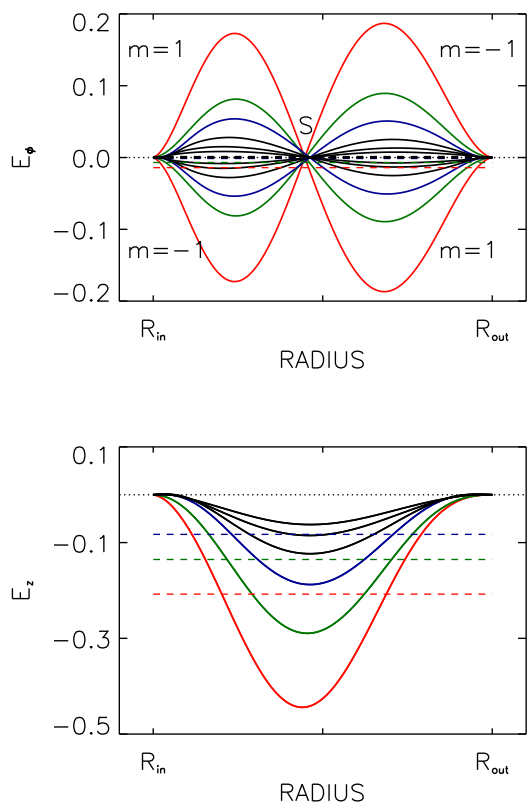


**Figure 4.** Normalized electromotive force  $\mathcal{E}_\phi$  (top) and  $\mathcal{E}_z$  (bottom) along the line of neutral stability within rigidly-rotating  $z$ -pinches. It is  $\text{Re} = 0$ ,  $\text{Ha} = 35$  (no rotation, red),  $\text{Re}_{\text{max}} = 140$ ,  $\text{Ha} = 50$  (slow rigid rotation, green) and  $\text{Re}_{\text{max}} = 418$ ,  $\text{Ha} = 100$  (fast rigid rotation, blue). The horizontal dashed lines give the values averaged over the radius for  $m = 1$ . It is  $\mathcal{E}_\phi \rightarrow -\mathcal{E}_\phi$  and  $\mathcal{E}_z \rightarrow \mathcal{E}_z$  for  $m \rightarrow -m$ .  $r_{\text{in}} = 0.5$ ,  $\mu_B = 1/r_{\text{in}} = 2$ ,  $m = \pm 1$ . Perfect-conducting cylinder walls. – We shall call the profiles of the top panel for  $m = 1$  as the “sine-type”  $\alpha$  effect and for  $m = -1$  as the “minus-sine-type”. S denotes the zeros of the sine-profiles which do not depend on  $m$  and  $\text{Re}$ .  $\text{Pm} = 0.1$ .

as the result of a spontaneous parity braking or by use of strictly formulated initial conditions. If the initial conditions clearly favor one mode then only this one is excited. If the initial condition do not favor one of the two modes, the numerical noise will determine the dominant mode. Not necessarily the solutions consist of equal mixtures of both degenerated modes (Gellert et al. 2011; Chatterjee et al. 2011; Bonanno et al. 2012). In this case the isolated mode with  $m = 1$  possesses a finite helicity (even without rotation) which is the negative value of the helicity of the mode  $m = -1$ .

The  $z$ -component of the mean-field electromotive force in cylinder geometry is  $\mathcal{E}_z = \langle u_R b_\phi - u_\phi b_R \rangle$ . The radial and azimuthal components of flow and field are invariant against the transformation  $m \rightarrow -m$ . Both the azimuthal and axial components of  $\mathcal{E}$  for resting or rigidly rotating containers are given in Fig. 4 normalized with the maximal total energy  $\text{MAX}(\langle \mathbf{u}^2 + \mathbf{b}^2 / \mu_0 \rho \rangle)$ . For fixed  $m$  all curves for  $\mathcal{E}_\phi$  are *almost* antisymmetric with respect to the common zero marked by S. This is a direct consequence of the one-cell pattern of the instability in linear approximation. Always the radial components of  $\mathbf{u}$  and  $\mathbf{b}$  are symmetric with respect to S and the axial components are antisymmetric resulting in an

antisymmetric structure of  $\mathcal{E}_\phi$ . For fixed  $m$  the  $\mathcal{E}_\phi$  curve behaves antisymmetric with respect to  $m \rightarrow -m$  but the  $\mathcal{E}_z$  curve does not. Here the curves for  $m = 1$  and  $m = -1$  are identical and hence the eddy diffusivity  $\eta_T$  is a robust quantity. The negative-definite sign of  $\mathcal{E}_z$  will lead to the expected positive-definite sign of  $\eta_T$ .

#### 4.1 Alpha effect

Consider the components  $\mathcal{E}_\phi$  and  $\mathcal{E}_z$  of the electromotive force. The ratio of both quantities is free of arbitrary factors and/or normalizations. We write  $\varepsilon_\alpha = \mathcal{E}_\phi / \mathcal{E}_z$ , i.e.

$$\varepsilon_\alpha = \frac{\langle u_z b_R - u_R b_z \rangle}{\langle u_R b_\phi - u_\phi b_R \rangle}. \quad (11)$$

With  $\mathcal{E}_\phi = \alpha B_\phi$  and  $\mathcal{E}_z = -\eta_T \text{curl}_z \mathbf{B}$  one immediately finds  $\varepsilon_\alpha = C_\alpha^{\text{sim}} / 2$ , where the standard notation

$$C_\alpha^{\text{sim}} = \frac{\alpha R_{\text{in}}}{\eta_T} \quad (12)$$

has been used. For uniform  $\alpha$  effect the excitation of a large-scale dynamo in an axially unbounded resting cylinder needs  $C_\alpha > 1$  (Meinel 1990).

The radial profiles of the two  $\mathcal{E}$  components are given in Fig. 4 for the stationary pinch (red lines) and the rigidly rotating pinch (green and blue lines) for marginal stability, for  $\text{Pm} = 0.1$  and for the modes with  $m = \pm 1$ . Averaged over  $\phi$  and  $z$  (defining cylindrical surfaces) the  $\mathcal{E}_\phi$  is sinusoidal. S denotes the nulls of the quasi-sine-profiles which are shown as independent of  $m$  and  $\text{Re}$ . One also finds that the *radial* average of the  $\mathcal{E}_\phi$  does not vanish as the amplitudes of the outer parts of the curves slightly exceed those of the inner parts. Averaged over the entire container, therefore, the  $\mathcal{E}_\phi$  is uniform but small with opposite signs for  $m = 1$  and  $m = -1$ . It is  $C_\alpha = O(0.1)$  if averaged over the whole container. The blue lines in Fig. 4 hold for stronger magnetic fields with  $\text{Ha} = 100$  and Reynolds number  $\text{Re}_{\text{max}} = 418$ . The dashed lines represent the corresponding values as averaged over the entire container. Note that the influence of the global rotation is only weak. The dependence of  $C_\alpha$  on the radial distribution  $\mu_B$  is not yet known.

The ratio  $\varepsilon_\alpha$  identically vanishes if both spirals with  $m = 1$  and  $m = -1$  are excited with the same power. A finite  $\alpha$  effect exists if only one of these modes is excited. Figure 5 shows the simulated  $C_\alpha^{\text{sim}}$  along the lines of neutral stability for uniform rotation ( $\mu = 1$ , dashed lines) and quasi-Keplerian rotation ( $\mu = 0.35$ , solid lines) as functions of the maximal Reynolds number. The magnetic Prandtl number varies by four orders of magnitude between  $\text{Pm} = 0.1$  and  $\text{Pm} = 10^{-5}$ . For not too slow rotation the resulting  $C_\alpha^{\text{sim}}$  hardly depend on the magnetic Prandtl number, the rotation law *and* the Reynolds number. For Kepler rotation  $C_\alpha^{\text{sim}} \simeq 0.1 \dots 0.2$  is the characteristic result of the simulations. The rotational suppression proves to be surprisingly weak. The same holds for the  $\text{Pm}$ -dependency. The red lines in Fig. 5 also show that for  $\text{Pm} = 0.1$  the differential rotation produces  $C_\alpha^{\text{sim}}$  larger by a factor of two than for uniform rotation. For small  $\text{Pm}$  these differences are even reduced.

We find that without and with rotation the pinch-type instability possesses zero  $\alpha$  effect if all modes are taken into account but it possesses  $C_\alpha^{\text{sim}}$  values of  $O(0.1)$  if only one of the modes is considered. The simulated  $C_\alpha$  are not quenched by the rotation but the resting  $z$ -pinch possesses slightly larger normalized  $\alpha$  effect than the rotating one.

It remains to ask whether the dynamo excitation is more

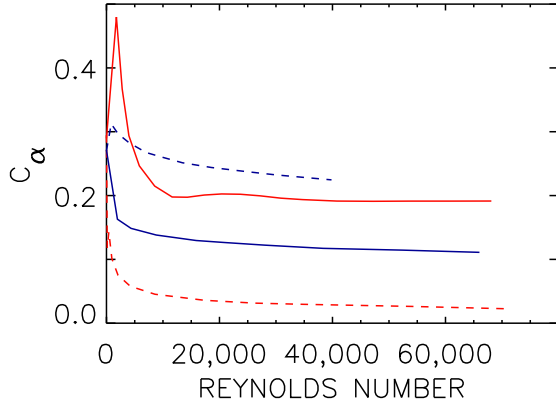


**Figure 5.** Simulation results of  $C_\alpha^{\text{sim}}$  averaged over the entire container for rigid rotation ( $\mu = 1$ , dashed lines) and quasi-Keplerian rotation ( $\mu = 0.35$ , solid lines).  $\text{Pm} = 10^{-5}$  (blue) and  $\text{Pm} = 0.1$  (red).  $r_{\text{in}} = 0.5$ ,  $\mu_B = 2$ ,  $m = -1$ . Perfect-conducting cylinder walls.

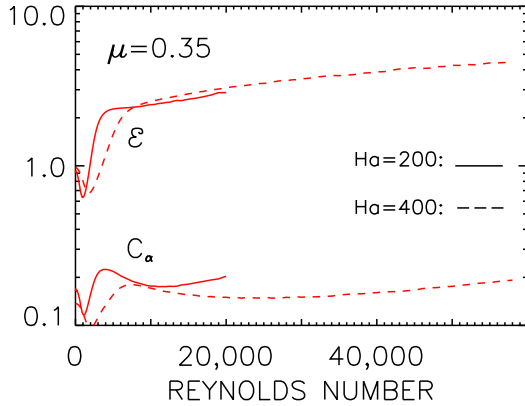


**Figure 6.** The normalized  $\alpha$  effect  $C_\alpha^{\text{sim}}$  and the energy ratio  $\varepsilon$  along a vertical line in the stability map (Fig. 1) for two given Hartmann numbers. It is always  $0 \leq \text{Re} \leq \text{Re}_{\text{max}}$ . Quasi-Keplerian rotation,  $\mu = 0.35$ .  $\text{Pm} = 0.1$ , perfect-conducting walls.

easy for fixed Hartmann number but for slower rotation, i.e. for  $\text{Re} < \text{Re}_{\text{max}}$ . The calculations along vertical lines in the stability map of Fig. 1 are much more complicated than they are along the line of neutral instability. For  $0 \leq \text{Re} < \text{Re}_{\text{max}}$  (at given  $\text{Ha}$ ) the growth rates of the magnetic instability are finite. The wave numbers and the drift frequencies must be optimized to find the maximal growth rates. The eigensolutions have been computed for exactly these values. We note that the absolute maximum of the growth rate exists for very small Reynolds numbers where  $\alpha\Omega$  dynamos do certainly not exist. Also vertical slices through the instability domain do not provide strong dependencies of the simulated  $C_\alpha$  on the Reynolds number (Fig. 6). The solid lines in this graph belong to  $\text{Ha} = 200$  while the dashed lines belong to  $\text{Ha} = 400$ . The result is that from a minimal Reynolds number on, the entire instability domain of Fig. 1 possesses more or less the same value of  $C_\alpha^{\text{sim}} = O(0.1)$ . Any mean-field dynamo theory might base on this basic result.

Also the energy ratio  $\varepsilon$  along the two vertical slices has been given in Fig. 6. The results are similar to those for the  $\alpha$  effect but for resting pinches there is a clear minimum with equipartition of the two energies. For increasing rotation the  $\varepsilon$  increases up to the values with  $b_{\text{rms}} > \sqrt{\mu_0\rho} u_{\text{rms}}$  which is already known for  $\text{Re} = \text{Re}_{\text{max}}$  (Fig. 3). Obviously, the numbers derived for the line of neutral instability well represent the numbers valid for the entire instability domain.

## 4.2 Eddy diffusivity

We shall turn now to the axial component of the electromotive force normalized with the kinetic and magnetic energies, i.e.

$$\varepsilon_z = \frac{\langle u_R b_\phi - u_\phi b_R \rangle}{\sqrt{\langle \mathbf{u}^2 \rangle \langle \mathbf{b}^2 \rangle}}. \quad (13)$$

Nominator and denominator are of the same dimension. This ratio can be computed with the quasilinear code in the same way as described above. It is always negative and does hardly depend on the rotation law. The dependence on the magnetic Prandtl number is  $\varepsilon_z \propto \text{Pm}^{-1/2}$  (except for  $\text{Re} = 0$ ).

Replacing the nominator in Eq. (13) by means of the diffusion approximation one finds with (10)

$$\eta_T = -\frac{\varepsilon_z}{2} \sqrt{\mu_0\rho} \langle \mathbf{u}^2 \rangle \frac{R_{\text{in}}}{B_{\text{in}}}. \quad (14)$$

Transformed to code units via  $\mathbf{u} = \hat{\mathbf{u}} \eta/D$  to magnetic Reynolds numbers one obtains

$$\frac{\eta_T}{\eta} = \frac{\sqrt{\varepsilon_z^2 \varepsilon}}{2S} \hat{u}_{\text{rms}}^2 \quad (15)$$

with  $\hat{u}_{\text{rms}} = \sqrt{\langle \hat{\mathbf{u}}^2 \rangle}$  as the turbulence velocity in code units. The magnetic energy of the perturbations does not explicitly contribute to the eddy diffusivity (Vainshtein & Kichatinov 1983). With the standard approximation  $\eta_T \simeq \tau_{\text{corr}} u_{\text{rms}}^2$  for an eddy diffusivity one finds the correlation time  $\tau_{\text{corr}}$  as

$$\tau_{\text{corr}} \simeq \frac{\sqrt{\varepsilon_z^2 \varepsilon}}{2} \frac{D}{V_A}, \quad (16)$$

which linearly scales with the magnetic turnover time  $D/V_A$  ( $V_A$  the Alfvén velocity of the toroidal field). The factor in front of  $D/V_A$  in (16) with 0.01...0.1 is only small with a very weak variation with the magnetic Prandtl number. The factor at the r.h.s. side of Eq. (15) can also be understood as a normalized correlation time,

$$\hat{\tau}_{\text{corr}} \simeq \frac{\sqrt{\varepsilon_z^2 \varepsilon}}{2S}. \quad (17)$$

The ratios  $\varepsilon$  and  $\varepsilon_z$  have numerically been calculated for several fixed Hartmann numbers in its dependence on the rotation rate and then combined to  $\hat{\tau}_{\text{corr}}$  (Fig. 7). The curves end at  $\text{Re} = \text{Re}_{\text{max}}$  where  $\hat{\tau}_{\text{corr}} S \simeq 0.02$ . The correlation time decreases for faster rotation, it varies by one or two orders of magnitudes. The results indicate that the eddy diffusivity for given Hartmann number close to the line with  $\text{Re} = \text{Re}_{\text{max}}$  is basically smaller than for slow rotation. Without rotation one finds  $\hat{\tau}_{\text{corr}} S \simeq 0.3$  independent of the magnetic Prandtl number.

Only a nonlinear 3D MHD code can provide the turbulence intensity  $\langle \mathbf{u}^2 \rangle$  in its dependencies on the rotation and the magnetic field. Below we shall see that just this dependence decides whether the instability can work as a dynamo or not. In a first approximation, the turbulence intensity may be estimated with the following argument. Let us only consider – as is often assumed in dynamo



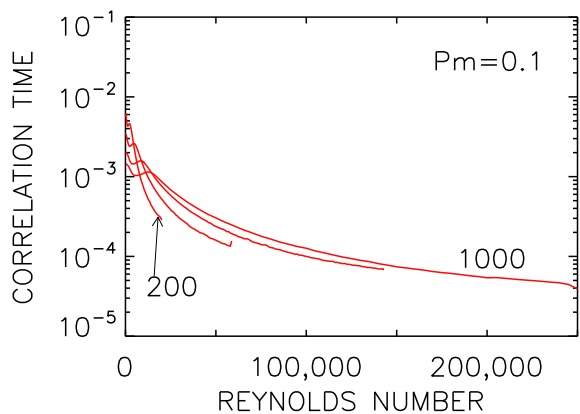


**Figure 7.** Simulation results of the correlation time  $\hat{\tau}_{\text{corr}}$  for quasi-Keplerian rotation. Four fixed Hartmann numbers  $\text{Ha} = 200$ ,  $\text{Ha} = 400$ ,  $\text{Ha} = 700$ ,  $\text{Ha} = 1000$ , as marked.  $\mu = 0.35$ ,  $\text{Pm} = 0.1$ . Perfect-conducting cylinder walls.

theory – those containers where the turbulence is in equilibrium with the applied magnetic field, i.e.  $\mu_0 \rho u_{\text{rms}}^2 = \kappa_{\text{eq}} B_{\text{in}}^2$ , with a dilution factor  $\kappa_{\text{eq}} \leq 1$ , hence

$$\frac{\eta_{\text{T}}}{\eta} = \hat{\tau}_{\text{corr}} \kappa_{\text{eq}} S^2, \quad (18)$$

which leads to a *linear dependence* of the eddy diffusivity on the magnetic field. Figure 7 also demonstrates a clear rotational decay of the correlation time. We note that numerical simulations of the magnetic diffusivity for quasi-Keplerian rotation and for a variety of magnetic Prandtl numbers indeed for large  $S$  lead to  $\eta_{\text{T}}/\eta \lesssim S/10$  (Rüdiger et al. 2018).

A more detailed turbulence model results from direct numerical simulations of the pinch-type instability with a nonlinear MHD code. The turbulence intensity  $u_{\text{rms}}^2$  depends on the magnetic field and the rotation rate. Here we shall only use the  $S$  dependence while the rotation dependence is still ignored. One finds a steep growth of the turbulence intensity with  $S$ , i.e.

$$\hat{u}_{\text{rms}}^2 = \kappa S^4. \quad (19)$$

To date the relation (19) is only known for the lowest possible Lundquist numbers. One finds

$$\frac{\eta_{\text{T}}}{\eta} = \hat{\tau}_{\text{corr}} \kappa S^4. \quad (20)$$

The  $\kappa$  defines that Lundquist number  $S_1$  where  $\eta_{\text{T}}/\eta = 1$ . Preliminary nonlinear simulations by Rüdiger et al. (2018) led to  $S_1 \simeq 100$  so that from (20)  $\kappa \simeq 5 \cdot 10^{-5}$  results. The specific eddy diffusivity exceeds unity if  $S > S_1$ . There the ratio of  $u_{\text{rms}}$  to the linear rotation velocity of the cylinder is a few percent. Only for even stronger magnetic fields  $\eta_{\text{T}}/\eta \gg 1$  is possible.

In this model the eddy diffusivity grows rapidly as  $S^3$  with the magnetic field amplitude. Also the Tayler-Spruit dynamo model in its original formulation works with an eddy diffusivity growing cubic with the magnetic background field and decaying with  $\Omega^{-1}$  (Spruit 2002).

## 5 DYNAMO EQUATIONS

The possibility will now be checked whether the perturbation patterns of the Tayler instability in combination with differential rotation may work as a dynamo leading to an axisymmetric large-scale magnetic field with dominating azimuthal component. The model of the rotating  $z$ -pinch may be the most simple one with which this problem can be attacked. To consider dynamo action for more complicated models is certainly more complicated.

The mean-field dynamo equation is

$$\frac{\partial \mathbf{B}}{\partial t} = \text{curl}(\alpha \cdot \mathbf{B} + \mathbf{U} \times \mathbf{B}) + (\eta + \eta_{\text{T}}) \Delta \mathbf{B}. \quad (21)$$

The quantities  $\alpha$  and  $\eta_{\text{T}}$  are derived by an averaging over time and space,  $\eta + \eta_{\text{T}}$  is assumed as uniform. As in contrast to convection the eddy resistivity  $\eta_{\text{T}}$  by magnetic instabilities is not necessarily large compared to  $\eta$  we have left the molecular resistivity in the mean-field equation (21). It shall be solved with the divergence-free ansatz  $\mathbf{B} = \text{curl}(A(R, z)\mathbf{e}_\phi) + B(R, z)\mathbf{e}_\phi$  for axisymmetric large-scale fields. The vector  $\mathbf{e}_\phi$  is the unit vector in azimuthal direction. The temporal and also the  $z$ -dependence for both components  $A$  and  $B$  are considered in the Fourier space, i.e. they are assumed as proportionate to  $\exp i(\omega t + Kz)$ . The real part of  $\omega$  is the cycle frequency of the dynamo. In order to have established a mean-field dynamo the resulting wave number  $K$  must be smaller than  $1/D$ .

The special case  $K = 0$  describes a dynamo without any  $z$  dependence. Then the radial field  $B_R = -iKA$  identically vanishes. In this case the differential rotation cannot induce new field components and the  $\Omega$  term in the dynamo equation vanishes. For  $K = 0$ , therefore, only  $\alpha^2$  dynamos can exist. The question is thus whether axially-periodic dynamos operate for finite values of the wave numbers  $K$  so that the  $\alpha^2$  dynamo type becomes an  $\alpha\Omega$  dynamo type which is even able to operate (for fast rotation) with rather weak  $\alpha$  effect. The equations for  $A(R)$  and  $B(R)$  are

$$\frac{d^2 A}{dR^2} + \frac{1}{R} \frac{dA}{dR} - \frac{A}{R^2} - (i\omega + K^2)A + C_\alpha \hat{\alpha} B = 0 \quad (22)$$

for the poloidal field component and

$$\begin{aligned} \frac{d^2 B}{dR^2} + \frac{1}{R} \frac{dB}{dR} - \frac{B}{R^2} - (i\omega + K^2)B + \hat{\alpha} C_\alpha K^2 A - \\ - C_\alpha \frac{d}{dR} \left( \hat{\alpha} \left( \frac{dA}{dR} + \frac{A}{R} \right) \right) - iKC_\Omega R \frac{d\hat{\Omega}}{dR} A = 0 \end{aligned} \quad (23)$$

for the toroidal component. Length scales have been normalized by the gap width  $D$ , frequencies with the diffusion frequency  $(\eta_{\text{T}} + \eta)/D^2$  and the normalized wave number is  $DK$ . The profiles  $\hat{\alpha}$  and  $\hat{\Omega}$  are normalized to unity.  $C_\alpha$  has been defined with (12) as  $C_\alpha = C_\alpha^{\text{sim}}/(1 + (\eta/\eta_{\text{T}}))$  and  $C_\Omega$  is the standard magnetic Reynolds number of rotation,  $C_\Omega = \Omega_{\text{in}} D^2 / (\eta + \eta_{\text{T}})$ . One can thus write

$$C_\alpha^{\text{sim}} = \left( 1 + \frac{\eta}{\eta_{\text{T}}} \right) C_\alpha, \quad \text{Rm} = \left( 1 + \frac{\eta_{\text{T}}}{\eta} \right) C_\Omega, \quad (24)$$

hence  $C_\alpha < C_\alpha^{\text{sim}}$  and  $\text{Rm} > C_\Omega$ . For  $\alpha\Omega$  dynamos with  $C_\Omega \gg C_\alpha$  only the product

$$\mathcal{D} = C_\alpha C_\Omega \quad (25)$$

forms the relevant eigenvalue indicating that dynamos are possible even for small  $\alpha$  if only the rotation is fast enough.

### 5.1 Boundary conditions

For perfectly conducting cylinders the boundary conditions are

$$A = 0, \quad \frac{dB}{dR} + \frac{B}{R} - C_\alpha \hat{\alpha} \left( \frac{dA}{dR} + \frac{A}{R} \right) = 0 \quad (26)$$

at  $R = R_{\text{in}}$  and  $R = R_{\text{out}}$ . The first condition ensures the vanishing of the radial magnetic field inside the inner cylinder and outside the outer cylinder while the second condition produces zero tangential component of the electromotive force. Pseudovacuum conditions (also called vertical field conditions) would require  $dA/dR + A/R = B = 0$  at  $R = R_{\text{in}}$  and  $R = R_{\text{out}}$  (Jackson et al. 2014). For more heuristic dynamo models also the simplified conditions  $B_R = B_\phi = 0$ , i.e.  $A = B = 0$ , have been used (Roberts 1972).

We shall also solve the dynamo equations (22) and (23) with the insulating boundary conditions, i.e. with (6) and (7) taken for  $m = 0$ , i.e.

$$\left( \frac{I_1(KR)}{I_0(KR)} - KR \right) A + \frac{I_1(KR)}{I_0(KR)} R \frac{dA}{dR} = 0, \quad B = 0 \quad (27)$$

for  $R = R_{\text{in}}$ , and

$$\left( \frac{K_1(KR)}{K_0(KR)} + KR \right) A + \frac{K_1(KR)}{K_0(KR)} R \frac{dA}{dR} = 0, \quad B = 0 \quad (28)$$

for  $R = R_{\text{out}}$ . Again  $I_m$  and  $K_m$  are the modified Bessel functions of second kind.

### 5.2 An analytical model

For uniform  $\alpha$  effect ( $\hat{\alpha} = 1$ ) in a resting container and for  $\omega = 0$  a stationary analytic solution  $B = C_\alpha A$  of Eqs. (22) and (23) exists if

$$\frac{d^2 A}{dR^2} + \frac{1}{R} \frac{dA}{dR} + (\tilde{C}_\alpha^2 - \frac{1}{R^2}) A = 0 \quad (29)$$

possesses an eigenvalue where  $\tilde{C}_\alpha^2 = C_\alpha^2 - K^2 > 0$  (Meinel 1990). The boundary condition  $A = 0$  at  $R_{\text{in}}$  and  $R_{\text{out}}$  from Eq. (26) are used (which also means  $B = 0$ ) producing the eigenequation

$$J_1(\tilde{C}_\alpha) Y_1(\tilde{C}_\alpha/r_{\text{in}}) - J_1(\tilde{C}_\alpha/r_{\text{in}}) Y_1(\tilde{C}_\alpha) = 0, \quad (30)$$

where  $J_1$  and  $Y_1$  are the Bessel functions of first kind with index  $m = 1$ . The  $Y_n$  are also called the Neumann-Weber functions. For  $r_{\text{in}} = 0.5$  one obtains from (30) the approximative eigenvalue  $\tilde{C}_\alpha \approx \pm\pi$ . The numerically derived exact value is  $\tilde{C}_\alpha = \pm 3.17$  hence  $C_\alpha = \sqrt{10.05 + K^2}$  so that  $C_\alpha$  grows with growing wave number. The axially homogeneous dynamo without axial bounds is obviously easiest to excite. The corresponding kinematic dynamo field is stationary, axisymmetric and helical. This analytical solution, however, is only of academic interest as the simulated  $\alpha$  effect averaged over the container is much smaller than  $C_\alpha = O(\pi)$  required for the cylindrical  $\alpha^2$  dynamo.

### 5.3 Numerical solutions

The numerical solutions of the equations (22) and (23) for infinite cylinders with finite  $C_\Omega$  have been obtained for three different radial  $\alpha$  profiles. Quasi-Keplerian rotation with  $\mu = 0.35$  for  $r_{\text{in}} = 0.5$  is always used. The upper panel of Fig. 8 gives for insulating boundary conditions the eigenvalues  $C_\alpha$  as function of the wave number and the normalized rotation rate  $C_\Omega$ . We note the choice  $\alpha = -1$ . Reynolds number  $C_\Omega$  of rotation and

wave number  $K$  are the free model parameters. The curves are marked with their value of  $C_\Omega$ . For  $C_\Omega = 0$  the analytical solution  $C_\alpha = \sqrt{10.05 + K^2}$  is well approximated where  $K = 0$  produces the minimal  $C_\alpha$ . For slow rotation ( $C_\Omega \lesssim 10$ ) the influence of the differential rotation is only weak and the  $C_\alpha$  slightly grows with growing wave number. For larger  $C_\Omega$  the eigenvalue  $C_\alpha$  sinks with growing wave number and possesses minima moving to smaller  $K$  for faster rotation. For  $C_\Omega = 1000$  the minimum value is  $C_\alpha \simeq 0.13$ . The dynamo numbers taken at the minimum thus converge to  $\mathcal{D} = 130$ .

The lower panel of Fig. 8 presents the cycle frequency  $\omega^{\text{R}}$  of the dynamo normalized with the magnetic-dissipation frequency  $(\eta_{\text{T}} + \eta)/D^2$ . The sign of this quantity depends on the sign of the  $\alpha$  effect, it is positive for negative  $\alpha$ . For vanishing  $K$  the dynamo turns into an  $\alpha^2$  dynamo which does not oscillate. It oscillates, however, already for slow differential rotation with  $C_\Omega = 10$ . For faster rotation the cycle frequency slightly grows. The frequency always exceeds the dissipation frequency but in all cases the ratio  $\omega^{\text{R}}/C_\Omega$  (which gives the dynamo frequency in units of the rotation rate) is small. Drift rates and growth rates of the magnetic instabilities always scale with the rotation rate. If the dynamo exists then the drift of the instability pattern of Tayler instability is short compared with the cycle frequency, at least for  $C_\Omega \gtrsim 100$ .

In order to model zeros of the  $\alpha$  effect at the walls the dynamo model has been modified by use of a half sine-type profile so that the  $\alpha$  is positive or negative throughout the gap and the maximum lies in the gap center. The upper panel of Fig. 9 shows the resulting numbers  $\mathcal{D}$  obtained for both sorts of boundary conditions. For vacuum conditions the eigenvalues are similar to those for uniform  $\alpha$ . The oscillation frequencies for positive  $\alpha$  have the opposite sign than those for negative  $\alpha$  (see Fig. 8). Most striking, however, is the behavior of the eigenvalues for the models with perfect-conducting cylinders. Here the minimum wave number is much smaller than for vacuum boundary conditions. The field geometry becomes more and more two-dimensionally. For  $K = 0$  the induction of the differential rotation vanishes and only a non-oscillating  $\alpha^2$  dynamo survives.

With Fig. 4 we have offered a sinusoidal  $\alpha$  effect for small Pm if only one mode is excited. The  $\alpha$  profile possesses a zero in the gap center and positive as well as negative values along the radius. Whether the inner part of the gap has positive or negative sign only depends on the mode considered with  $m = 1$  or  $m = -1$ . The critical  $C_\alpha$  for the  $\alpha^2$  dynamo must thus be expected as basically higher than 3.17. For both sorts of sinusoidal  $\alpha$  effect the critical value of  $C_\alpha$  for  $\alpha^2$  dynamos is  $C_\alpha = 4.85$  for conducting boundaries and  $C_\alpha = 4.91$  for insulating boundaries. Because of the small values of the simulated  $C_\alpha^{\text{sim}} < 1$  an  $\alpha^2$  dynamo on basis of the Tayler instability can therefore not exist.

For slow rotation the dynamo is stationary while it oscillates for faster rotation. The normalized frequencies are very similar to the numbers in the lower panel of Fig. 8. There is no visible influence of the form of the radial profile of the  $\alpha$  effect. The lower panel of Fig. 9 demonstrates that again the dynamo number  $\mathcal{D}$  for conducting walls is smaller than for insulating walls. The minimum value for the model with the vacuum boundary conditions for the sine-type model results as  $\mathcal{D} \approx 700$  while for a quasi-uniform  $\alpha$  effect  $\mathcal{D} \approx 200$  results. With sufficiently large  $C_\Omega$  mean-field dynamos with very small  $C_\alpha$  are always possible. From Eqs. (24) and (25) one obtains

$$C_\alpha^{\text{sim}} \text{Rm} \gtrsim \mathcal{D} \left( 1 + \frac{\eta}{\eta_{\text{T}}} \right) \left( 1 + \frac{\eta_{\text{T}}}{\eta} \right) \quad (31)$$



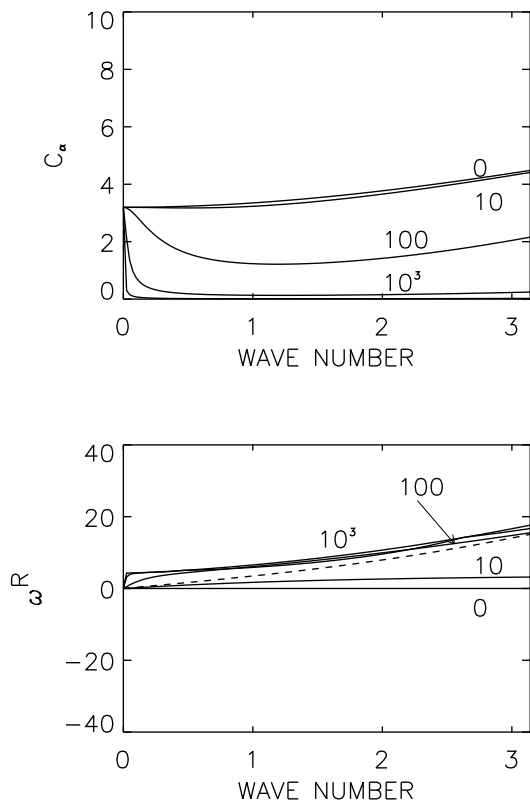


**Figure 8.** Eigenvalues  $C_\alpha$  (top) and drift frequencies (bottom) of  $\alpha^2\Omega$  dynamos with quasi-Keplerian rotation for insulating walls and uniform  $\alpha$  profile. The curves are marked with their values of  $C_\Omega$ .  $r_{\text{in}} = 0.5$ ,  $\mu = 0.35$ .

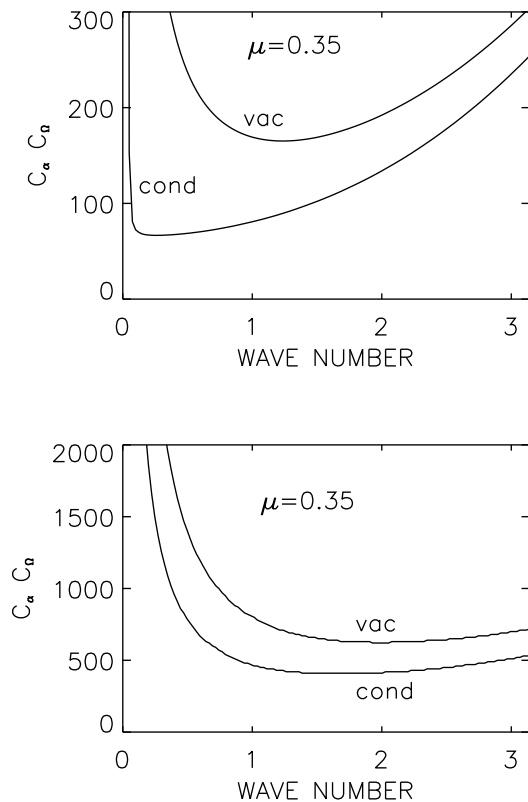


**Figure 9.** Dynamo number  $\mathcal{D} = C_\alpha C_\Omega$  for non-uniform  $\alpha$  profiles and quasi-Keplerian rotation law. Top: half sine-type  $\alpha$  profile (no sign change between  $R_{\text{in}}$  and  $R_{\text{out}}$ ), bottom: sine-type  $\alpha$  profile (one sign change of  $\alpha$  between  $R_{\text{in}}$  and  $R_{\text{out}}$ ).  $C_\Omega = 1000$ ,  $r_{\text{in}} = 0.5$ ,  $\mu = 0.35$ . Insulating (vac) and perfect-conducting (cond) cylinder walls.

as the dynamo condition where the right-hand side of this relation always equals or even exceeds  $4\mathcal{D}$ . Obviously, with uniform  $\alpha$  effect for  $\text{Rm} < \text{Rm}_{\text{crit}}$  with  $\text{Rm}_{\text{crit}} = 4\mathcal{D}/C_\alpha^{\text{sim}}$  no dynamo excitation is possible. On the other hand, this relation also means  $\text{Re} \rightarrow \infty$  for  $\text{Pm} \rightarrow 0$  so that always a (small) magnetic Prandtl number exists below which even a hypothetical dynamo certainly decays. In that sense our attention is focused to models with (say)  $\text{Pm} = 0.1$ . For smaller  $\text{Pm}$  dynamo operation is even more complicated.

Whether for larger magnetic Reynolds numbers a dynamo can work or not depends on the details of the eddy diffusivity theory. The dynamo action is basically suppressed for  $\eta_T \gg \eta$  and also for  $\eta_T \ll \eta$ . If, however, a saturation of  $\eta_T/\eta$  for large  $\text{Rm}$  and/or  $S$  exists then the dynamo action is always possible for the resulting sufficiently large values of  $\text{Rm}$ . One finds that mainly the assumptions about  $\eta_T/\eta$  decide whether a Taylor dynamo mechanism may work.

Figure 9 (bottom) also demonstrates the existence of a minimum for the eigenvalue at  $K \simeq 1.5$  which is at least by a factor of two smaller than the vertical wave numbers  $k$  of the Taylor instability. For smaller  $K$  the shear effect in the dynamo is too small and for larger  $K$  the dissipation is too large.

## 6 DISCUSSION AND CONCLUSIONS

The stability of Taylor-Couette flows with conducting material has been discussed where an axial homogeneous current produces a toroidal magnetic background field. The rotation rates of the cylinders are prescribed; only solid-body and quasi-Keplerian rotation laws are here applied. A nonaxisymmetric Taylor instability appears in this model if the rotation is not too fast. For given (supercritical) Hartmann number always a maximal Reynolds number  $\text{Re}_{\text{max}}$  exists above which the fluid is stable.  $\text{Re}_{\text{max}}$  also depends on the magnetic Prandtl number,  $\text{Re}_{\text{max}} \propto \text{Pm}^{-0.16}$  for Kepler rotation and small  $\text{Pm}$ . The  $\text{Pm}$ -dependence disappears for Chandrasekhar-type flows, where the lines of marginal stability in the  $(\text{Ha}/\text{Re})$  plane do not depend on the (small) magnetic Prandtl number.

The eigenfunctions  $\mathbf{u}$  and  $\mathbf{b}$  have been computed by means of the linearized equations. The two Fourier modes with  $m = 1$  and  $m = -1$  of the instability are degenerated possessing identical critical Hartmann numbers and Reynolds numbers for excitation. Each of them is helical with opposite values of  $\langle \mathbf{u} \cdot \text{curl } \mathbf{u} \rangle$  and  $\langle \mathbf{b} \cdot \text{curl } \mathbf{b} \rangle$ . Both the total sums of the kinetic and magnetic helicity vanish. It is thus clear that in the mean-field formulation of

dynamo theory the  $\alpha$  effect vanishes if the two possible modes are coexisting<sup>1</sup>.

One can ask whether dynamo action is possible if only one of the modes is excited. Then kinetic and magnetic helicity exist even without rotation but these values are subcritical for dynamo action. Calculating the axial and the azimuthal components of the electromotive force with the eigenfunctions of the linearized equation system the normalized  $\alpha$  effect,  $C_\alpha$ , results without any free or unknown parameter. Its value never exceeds unity, and the dependences on the magnetic Prandtl number (for  $Pm \lesssim 1$ ) and the rotation rate are weak. Averaging over the entire container one obtains  $C_\alpha^{sim} = O(0.1)$  which is not large enough for the operation of an  $\alpha^2$  dynamo.

However, an  $\alpha\Omega$  dynamo with  $\alpha$  effect *and* differential rotation may work where – if the latter is only strong enough – the  $\alpha$  term can even be very weak. The resulting dynamo condition

$$Rm \geq \frac{D}{C_\alpha^{sim}} \left( 2 + \frac{\eta_T}{\eta} + \frac{\eta}{\eta_T} \right) \quad (32)$$

provides a lower limit of the magnetic Reynolds number for dynamo excitation of  $Rm_{crit} = 4D/C_\alpha^{sim}$  as the absolute minimum of the bracket expression is 4. From the upper panel of Fig. 9 we take  $D = 100$  for perfect-conducting boundaries as the most optimistic eigenvalue of dynamo excitation. On the other hand, the numerical value  $C_\alpha^{sim}$  remains nearly constant for all Reynolds numbers, magnetic Prandtl numbers and shear values (see Fig. 5) hence one finds dynamo excitation as only possible for  $Rm \gtrsim 2.000$ . This is a large value which excludes the possibility of related dynamo experiments with liquid metals in the laboratory. For  $Pm = 10^{-5}$  it is  $Re_{crit} = 4 \cdot 10^8$  below which dynamo excitation is excluded. Note also that for  $Pm \rightarrow 0$  the critical Reynolds number for dynamo action grows to infinite.

For  $Pm = 0.1$  the minimal Reynolds number for dynamo excitation is  $Re_{crit} \simeq 20.000$  which needs Hartmann numbers

$$Ha \geq Ha_{crit} \quad (33)$$

with  $Ha_{crit} = 207$  for quasi-Keplerian rotation<sup>2</sup>. For smaller Hartmann numbers it is always  $Re_{max} < Re_{crit}$  because of the rotational suppression of the Taylor instability. On the other hand, the critical Hartmann number lies slightly below the Hartmann number  $Ha_1 = S_1/\sqrt{Pm}$  which after (20) defines the magnetic field for which  $\eta_T = \eta$ . It is thus clear that close to the Hartmann number  $Ha_{crit}$  an  $\alpha\Omega$  dynamo may exist.

The relation (33) forms a *necessary* condition for dynamo excitation, the corresponding minimum Mach number for  $Pm = 0.1$  is  $Mm \simeq 30$ . The values are obviously too large for the numerical simulation of the magneto-turbulence in Taylor-Couette flows. We have thus to work with simplified models to provide eddy diffusivity values in dependence on the applied (large) Reynolds numbers. Let us first numerically study the dynamo condition in the form

$$\chi = \frac{D}{C_\alpha^{sim} Rm} \left( 2 + \frac{\eta_T}{\eta} + \frac{\eta}{\eta_T} \right) \leq 1. \quad (34)$$

As the numerical value of  $C_\alpha$  does hardly depend on the Reynolds number and the magnetic Prandtl number, it is thus clear that mainly the ratio  $\eta_T/\eta$  decides about dynamo excitation or not. Both

<sup>1</sup> Because of the topology of the model also the  $\Omega \times \mathbf{J}$  term of the turbulence electromotive force vanishes.

<sup>2</sup> For example: a pinch current of 50 kA with  $r_{in} = 0.5$  generates Hartmann numbers of  $Ha = 129$  for GaInSn and  $Ha = 406$  for liquid sodium, resp.

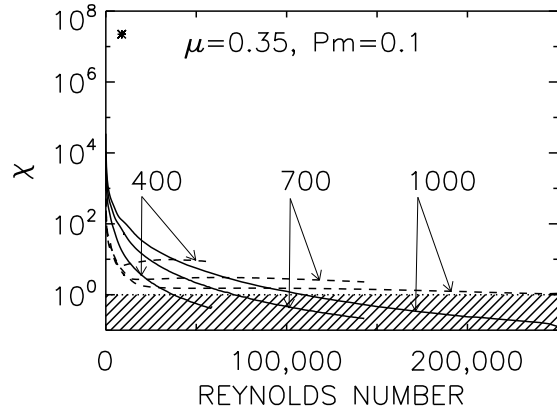


**Figure 10.** Ratio  $\chi$  for magnetic-equilibrated turbulence with  $D = 100$  for quasi-Keplerian rotation and for three different Hartmann numbers (marked). Each curve ends with its maximal Reynolds number  $Re_{max}$ . Solid lines:  $\kappa_{eq} = 1$ , dashed lines:  $\kappa_{eq} = 0.005$ . Dynamo self-excitation ( $\chi \leq 1$ , shaded area) is only possible for large Reynolds numbers (i.e.  $Mm \gtrsim 30$ ) and for  $\kappa_{eq} > 0.005$ . The asterisk represents a model with  $Pm = 10^{-5}$  for  $Ha = 50$  and  $Re_{max} = 8812$ .  $r_{in} = 0.5$ ,  $\mu_B = 2$ ,  $\mu = 0.35$ ,  $Pm = 0.1$ . Perfect-conducting cylinder walls.

large and also small values of  $\eta_T/\eta$  hinder the dynamo excitation. If  $\eta_T/\eta$  is independent of  $Rm$  and/or  $S$  – or if by saturation a maximal value exists – then always a (large)  $Rm \geq Rm_{crit}$  exists for which  $\chi$  becomes small enough so that the dynamo condition is fulfilled. For  $Rm < Rm_{crit}$  the condition (34) can never be fulfilled. That the possible existence of dynamo action depends on the details about the instability-induced diffusivity bases on the two features of the Taylor instability that i) the simulated  $C_\alpha^{sim}$  is nearly constant for all magnetic fields and rotation rates and that ii) the rotation rate has a maximal value which cannot be exceeded unless the instability decays.

If the  $\eta_T/\eta$  grows *linearly* with the Lundquist number  $S$  then the numerical values of the parameters (including the magnetic Mach number) decide whether the dynamo condition is fulfilled or not. Figure 10 demonstrates for the quasi-linear model defined by Eq. (18) that for  $Ha \geq 400$  dynamo solutions always exist (if  $\kappa_{eq} = 1$ ). The  $\chi$ 's take their minimum for the largest Reynolds numbers  $Re_{max}$ . Only rapidly rotating containers can thus be dynamo-active. Here the  $Re_{max}$  (above which the Taylor instability decays) is large enough to fulfill the condition (34). The magnetic Mach number must exceed a critical value (here  $Mm \simeq 10$ ), which for quasi-Keplerian rotation and the chosen magnetic Prandtl number (here  $Pm = 0.1$ ) is always possible.

It is  $\eta_T > \eta$  along all curves with  $\kappa_{eq} = 1$  in Fig. 10. Because of the rotational suppression of the correlation time  $\tau_{corr}$  shown in Fig. 7 the fast-rotation parts of the curves possess much smaller eddy diffusivities than their slow-rotating parts. Only the fast-rotating parts are located in the dashed areas of dynamo self-excitation. It is also obvious that models with  $\kappa_{eq} < 1$  are even more dynamo-active than the plotted examples with  $\kappa_{eq} = 1$ . The effective Mach number in this case is increased. For too small  $\kappa_{eq}$ , however, the eddy diffusivity becomes smaller than the microscopic one and the bracket in (32) becomes large enough to suppress the dynamo. The smallest possible  $\kappa_{eq}$  for dynamo self-excitation of the examples shown in Fig. 10 is 0.005. Obviously, the dynamo-instability of this model is rather robust.

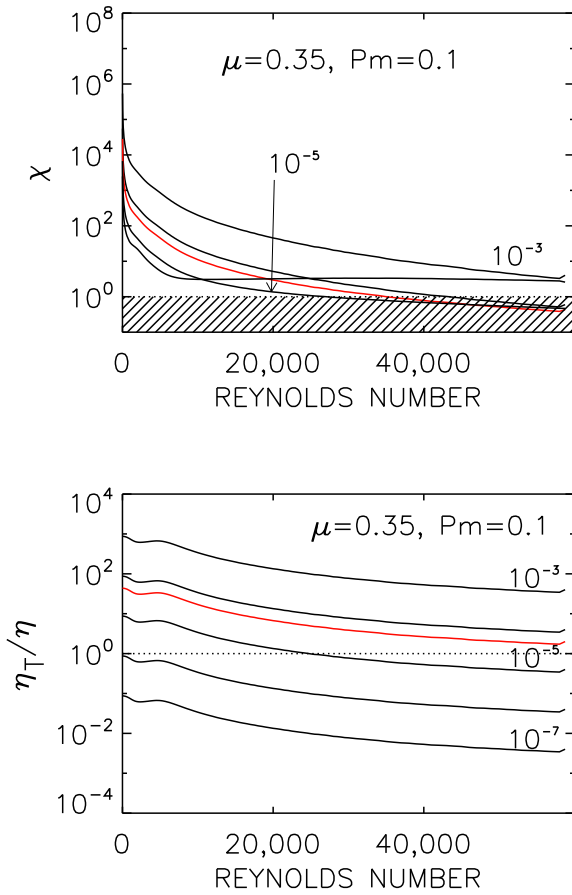


**Figure 11.** Similar as Fig. 10 but for the nonlinear turbulence model (19) for fixed Hartmann number  $Ha = 400$  for all  $Re \leq Re_{max}$ .  $\kappa$  (marked) is uniform between  $R_{in}$  and  $R_{out}$ . Top panel: ratio  $\chi$ , bottom panel: ratio  $\eta_T/\eta$ . The horizontal dotted line gives  $\eta_T = \eta$ . The red lines belong to  $\kappa = 5 \cdot 10^{-5}$ .  $\mathcal{D} = 100$ ,  $r_{in} = 0.5$ ,  $Pm = 0.1$ ,  $\mu = 0.35$ . Perfect-conducting cylinder walls.

We shall proceed with a diffusivity model for which the diffusivity grows faster with the magnetic field. In this case the dynamo condition (34) should also have limits where the magnetic diffusivity is too large for dynamo excitation. The highly nonlinear model (19) is applied. We note that along the “vertical slices” in the  $(Ha/Re)$  plane the growth rates of the instability are positive for  $Re < Re_{max}$ . We note that their maxima for fixed  $Ha$  exist at small Reynolds numbers shortly above the horizontal axis where  $\alpha\Omega$  dynamos do certainly not exist.

Figure 11 gives the function  $\chi$  defined by (34) for  $Ha = 400$  and various  $\kappa$ . The Hartmann number exceeds the minimum value (33) so that dynamo solutions are not basically excluded. The top panel of this figure shows the excitation conditions while the bottom panel gives the corresponding diffusivity values  $\eta_T/\eta$ . We find dynamo excitation with the lowest Reynolds number for  $\kappa = 10^{-5}$ . The eddy diffusivity for this  $\kappa$  value is of order unity. The larger value  $\kappa = 5 \cdot 10^{-5}$  known from Section 4.2 for for  $Ha_1 = 316$  also leads to dynamo excitation with somewhat higher value of  $\eta_T/\eta$ . For the smaller value  $\kappa = 10^{-6}$  the eddy diffusivity is too small for dynamo excitation. On the other hand, dynamo action does not appear for  $\kappa > 10^{-4}$ . The eddy diffusivity for lower or higher  $\kappa$

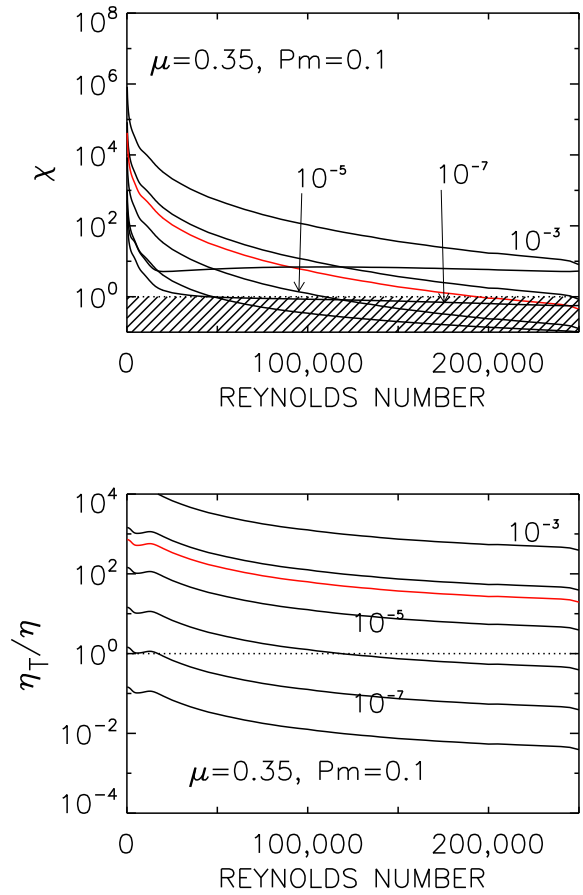


**Figure 12.** Similar as Fig. 11 but for  $Ha = 1000$  and all  $Re \leq Re_{max}$ .

values proves be too low or too high for the  $\alpha\Omega$  dynamo mechanism. Because of the existence of the upper limits  $Re_{max}$  of the Reynolds numbers the curves for  $\kappa > 10^{-4}$  in Fig. 11 (top) are not long enough to reach the shaded area.

Similar data for  $Ha = 1000$  are given by Fig. 12. One finds the excitation with the lowest Reynolds number for the smaller value  $\kappa = 10^{-6}$ . Again the specific eddy diffusivity for this  $\kappa$  value is of order unity. The larger value  $\kappa = 5 \cdot 10^{-5}$  (red line) moved upwards in comparison to Fig. 11; it will finally leave the shaded dynamo excitation area for  $Ha > 1000$  because of the increase of  $\eta_T/\eta$  for increasing Lundquist number. One also finds that for  $\kappa = 10^{-8}$  the eddy diffusivity is too small for dynamo excitation and for  $\kappa = 10^{-3}$  it is too large. Just for  $\eta_T = \eta$  the bracket in the dynamo condition (34) takes its lowest value hence the self-excitation is easiest. Again it is demonstrated by the upper panel of Fig. 12 that because of the existence of the maximal Reynolds number (here  $Re_{max} \simeq 250.000$ ) the curves for too small or too large  $\kappa$  are simply not long enough for dynamo excitation.

That the values of  $C_{\alpha}^{sim}$  are almost uniform in the entire instability domain does not mean that the  $\alpha$  effect and the eddy diffusivity are almost constant. We only know that their ratio is almost constant. For differentially rotating fluids an  $\alpha\Omega$  dynamo could exist but we find that the maximal possible rotation rates (defined by  $Re_{max}$ ) can easily be too slow to maintain the dynamo. On the other hand, the existence of large-scale dynamo action for solid-body rotation can be excluded with ease.

The influence of the magnetic Prandtl number on the dynamo excitation is still an open question. We also note that the  $\chi$  values drastically grow for smaller  $Pm$ . The asterisk in Fig. 10 represents an isolated calculation of a model with quasi-Keplerian rotation for  $Pm = 10^{-5}$  demonstrating the massive stabilization by small magnetic Prandtl numbers. As an example, the critical Reynolds number  $Re_{crit}$  allowing dynamo excitation for  $Pm = 10^{-5}$  is  $2 \cdot 10^8$ , which is far beyond our numerical limitations. The following argument goes in a similar direction. It is obvious that the  $Pm$ -dependence of the eddy-diffusivity determines the  $Pm$ -dependence in the dynamo condition (34). With numerical simulations Gellert & Rüdiger (2009) demonstrated that  $\eta_T/\eta$  for given Hartmann number does not depend on the magnetic Prandtl number, hence  $\eta_T/\eta \propto Ha$ , or similarly,  $\eta_T/\eta \propto S/\sqrt{Pm}$ . For large enough  $\eta_T/\eta$  the dynamo condition (34) turns into  $\chi \propto Mm^{-1}Pm^{-1/2}$  which for small  $Pm$  grows to large values.

There is thus an indication that small  $Pm$  suppresses the dynamo-instability of the Tayler pattern. The deeper reason of this phenomenon may be that the dynamo condition (32) basically scales with the magnetic Reynolds number while the rotational quenching of the Tayler instability scales with the ordinary Reynolds number which both strongly differ for small magnetic Prandtl numbers.

## 7 ACKNOWLEDGMENT

Frank Stefani from the Helmholtz-Zentrum Dresden-Rossendorf is acknowledged for many discussions and several critical readings of the manuscript.

## REFERENCES

- Bonanno A., Brandenburg A., Del Sordo F., Mitra D., 2012, *Physical Review E*, 86, 016313
- Braithwaite J., 2006, *Astronomy & Astrophysics*, 453, 687
- Chandrasekhar S., 1956, *Proc. Natl. Acad. Sci. USA*, 42, 273
- Chatterjee P., Mitra D., Brandenburg A., Rheinhardt M., 2011, *Physical Review E*, 84, 025403
- Gellert M., Rüdiger G., 2009, *Physical Review E*, 80, 046314
- Gellert M., Rüdiger G., Elstner D., 2008, *Astronomy & Astrophysics*, 479, L33
- Gellert M., Rüdiger G., Hollerbach R., 2011, *Month. Not. Roy. Astr. Soc.*, 414, 2696
- Goldstein J., Townsend R. H. D., Zweibel E. G., 2019, *The Astrophysical Journal*, 881, 66
- Guseva A., Hollerbach R., Willis A. P., Avila M., 2017, *Physical Review Letters*, 119, 164501
- Jackson A., Sheyko A., Marti P., Tilgner A., Cébron D., Vantieghem S., Simatev R., Busse F., Zhan X., Schubert G., Takehiro S., Sasaki Y., Hayashi Y.-Y., Ribeiro A., Nore C., Guermond J.-L., 2014, *Geophysical Journal International*, 196, 712
- Kirillov O. N., Stefani F., Fukumoto Y., 2012, *The Astrophysical Journal*, 756, 83
- Meinel R., 1990, *Geophysical and Astrophysical Fluid Dynamics*, 50, 79
- Pitts E., Tayler R. J., 1985, *Month. Not. Roy. Astr. Soc.*, 216, 139
- Rüdiger G., Gellert M., Hollerbach R., Schultz M., Stefani F., 2018, *Physics reports*, 741, 1
- Rüdiger G., Schultz M., Stefani F., Hollerbach R., 2018, *Geophysical and Astrophysical Fluid Dynamics*, 112, 301
- Seilmayer M., Stefani F., Gundrum T., Weier T., Gerbeth G., Gellert M., Rüdiger G., 2012, *Physical Review Letters*, 108, 244501
- Spruit H. C., 2002, *Astronomy & Astrophysics*, 381, 923
- Tayler R. J., 1957, *Proceedings of the Physical Society B*, 70, 31
- Tayler R. J., 1973, *Month. Not. Roy. Astr. Soc.*, 161, 365
- Vainshtein S. I., Kichatinov L. L., 1983, *Geophysical and Astrophysical Fluid Dynamics*, 24, 273
- Zahn J.-P., Brun A. S., Mathis S., 2007, *Astronomy & Astrophysics*, 474, 145